PAPER • **OPEN ACCESS**

Dynamic response of a single point mooring submersible fish cages in waves and current

To cite this article: X Wen *et al* 2023 *IOP Conf. Ser.: Mater. Sci. Eng.* **1294** 012013

Dynamic response of a single point mooring submersible fish cages in waves and current

X Wen*, H Cheng and M C Ong

Department of Mechanical and Structural Engineering and Materials Science
University of Stavanger, NO-4036, Stavanger, Norway

* Correspondence: xueliang.wen@uis.no

Abstract. Submersible fish cages are designed for installing in the open sea sites that are subjected to violent sea conditions to reduce the hydrodynamic forces acting on the fish cages. To assess the dynamic responses of a single point mooring submersible fish cage under the rough sea conditions, a numerical model including hydrodynamic and structural methods is proposed. The waves and current are modelled using the airy wave theory. For the floating collars and sinker tube, the Morison model is adopted to calculate the hydrodynamic force and the modal superposition method is proposed to calculate the structural responses. For the aquaculture net, the screen model is adopted to calculate the hydrodynamic force and the extended position-based dynamics (XPBD) method is proposed to obtain the structural deformations. The hydrodynamic dynamic forces and the deformations of the fish cages are compared between the fish cages on water surface and in deep water. Results show that when the fish cage is submerged 20m from the water surface, the average horizontal force is reduced by 30% and the variation of the horizontal force is reduced by 81%. Significant reductions in the deformation of the floating collars are observed. Therefore, using submersible fish cage can help reduce physical stress and avoid structural damage for the fish cage system. In addition, the coupling of XPBD and MS can provide a quick solution for the structural modelling of the fish farm system, which can be utilized at the initial stage of fish farm design.

1. Introduction

Aquaculture has been the world's fastest-growing food production method in the past 40 years [1]. Open sea aquaculture is a new development of the aquaculture industry because of the benefits of the fish welfare and the ecosystem through better water exchange and dispersal of waste [2]. However, it can pose a significant challenge to the design of open sea fish cages due to the strong waves and current in the open sea. Submersible fish cages were designed for installing in the open sea sites that are subjected to violent sea conditions to reduce the hydrodynamic forces acting on the fish cages. The cages are floated to the water surface when the sea is in calm condition. If the tidal currents and waves are strong when a furious storm or a typhoon is coming, the fish cage will descend to a specific position. This position is especially designed to minimize or avoid structural damage by reducing physical stress from the rough sea conditions. The descending is achieved by ballasting sea water into one of the floating collars and thus increasing the fish cage's weight. When the furious storm or the typhoon passes, the water inside the floating collar will be de-ballasted using a pump and high-pressure air. The fish cage

ascends to the water surface due to the decreasing of the weight of the fish cage. To design such a submersible fish cage system, an effective numerical method should be proposed to assess the dynamic responses of the fish cage under rough sea conditions of the typhoon or the furious storm. Besides, the descending and ascending of the fish cage are risky under the rough sea conditions when the typhoon or the furious storm is approaching. It is also necessary to evaluate the structural responses during the dynamic processes of the descending and ascending of the fish cage.

The numerical methods to assess the dynamic response of the fish cage include the hydrodynamic models and the structural models. For the hydrodynamic models, there are three types of hydrodynamic models for aquaculture nets: Morison model and screen model and porous media model. The Morison models were proposed to calculate the hydrodynamic force acting on line-like structures of the aquaculture nets [3-4]. The aquaculture nets are usually very dense. The twine length can be smaller than 2cm. The mesh number of the net for the Morrison model becomes quite extensive if each twine is modelled. A mesh grouping method was proposed by Cheng et al. [5] to reduce the mesh number of the net. In screen models, the hydrodynamic forces are calculated based on a number of net panels. The twines and knots in the net panel are considered as an integrated structure with a solidity representing the ratio of the twines' projected area to the total area of the net panel. In some screen models, the hydrodynamic force acting on the net panel is decomposed into two components: a normal drag force and a tangential drag force [6], dependent on the orientation of the net panel. In other models [7-8], the hydrodynamic force acting on the net panel is decomposed into a drag force and a lift force according to the direction of the flow passing the panel. The porous media models were adopted in the modelling of the aquaculture net in the computational fluid dynamics methods [9-10]. For the structural methods, various methods were proposed to assess the structural responses of different components of the fish cage system. A mass-spring model [11] or a truss model [12] was used to calculate the motions and deformations of the aquaculture nets, mooring lines and bridles. A rigid body model [13] or beam model [12] was adopted to model the motions and deformations of the floating collars and the sinker tubes.

In the present study, the dynamic responses of a single point mooring fish cage under rough sea conditions are assessed. The hydrodynamic models include a screen model proposed by Aarsnes et al. [7] to obtain the hydrodynamic forces acting on the net panels and a Morrison model to obtain the hydrodynamic forces acting the floating collars and sinker tube. The structural models include an extended position-based dynamics (XPBD) method [14-15] to model the structures of the aquaculture nets, mooring lines and bridles and a mode superposition method to model the floating collars and the sinker tubes. The hydrodynamic dynamic forces and the deformations of the fish cages are compared between the fish cage on surface and in deep water.

2. Numerical model

2.1 Description of the single point mooring submersible fish cage

The investigated single point mooring submersible fish cage system is shown in Figure 1. The fish cage has a circumference of 160 m and a total height of 35 m. There are two floating collars on the top of the fish cage, a sinker tube at the depth of 30m, a sinker of 5000 N (weight in water) at the depth of 35m and the net pens between them. The mooring system includes a buoy, an anchor, one mooring line and three bridles. The three bridles connect the fish cage and the buoy. The buoy is a combination of a cylinder and an inverse cone, which have a diameter of 2m. The heights of the cylinder part and cone part are 1m and 2m, respectively. The floating collars of the fish cage is initially located at the mean sea water level. The origin of the present coordinate system is set at the centre of the floating collars. The x-axis is along the direction of the current. The z-axis points vertically upward and the y-axis is given by satisfying the right-hand rule. The conjunction point between the mooring line and the three bridles is initially located at a depth of -10 m. The anchor is installed at the sea bottom with a depth of -100 m. The density of the sea water is 1025 kg/m^3 and the gravitational acceleration is 9.81 m/s^2.

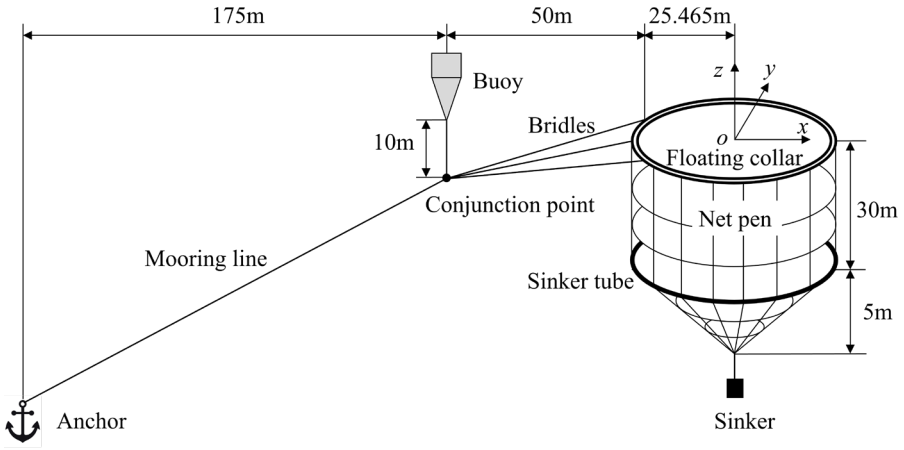

Figure 1. Schematic of a single point mooring fish cage.

Figure 2 shows the front, side and top views of the net pen as well as well as the description of the net twines and ropes. The frame of the net pen is made of net ropes and enclosed by the net ropes is net twines. The specifications of the single point mooring fish cage system are displayed in Table 1. The density and Young's modulus of different materials are listed in Table 2.

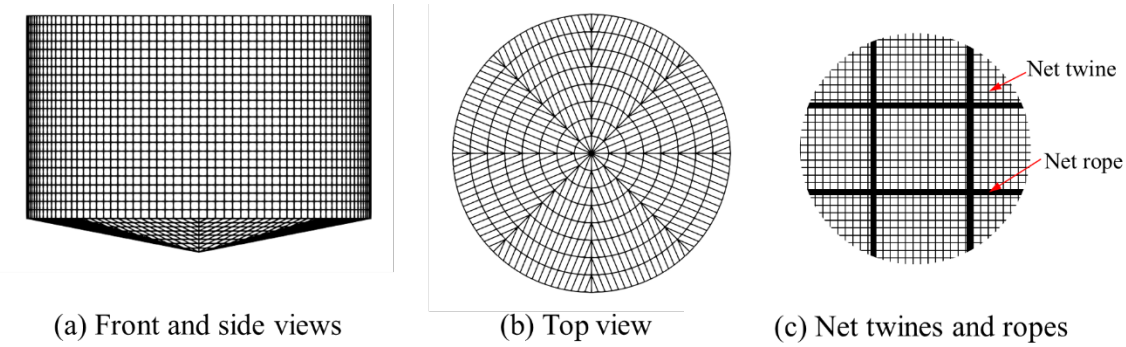

(a) Front and side views (b) Top view (c) Net twines and ropes

Figure 2. Front, side and top view of the net pen as well as the description of the net twines and ropes.

Table 1. Specifications of the single point mooring fish cage system.

Component	Parameter	Value
Net twine	Diameter	2.8 mm
	Mesh length	25 mm
	Solidity	0.2
	Material	Nylon
Net rope	Diameter	10mm
	Material	PE
Floating collar	Section diameter	355 mm
	Pipe thickness	21mm
	Material	HDPE
Sinker tube	Section diameter	250 mm
	Pipe thickness	21 mm
	Material	HDPE
Bridles	Diameter	100 mm
	Material	Nylon
Mooring line	Diameter	100 mm
	Material	Nylon

Table 2. Density and Young's modulus of different materials.

	Nylon	PE	HDPE
Density	1140 kg/m^3	960 kg/m^3	960 kg/m^3
Young's modulus	2.0 GPa	1.5 GPa	3.0 GPa

2.2 Hydrodynamic model

2.2.1 Current and wave conditions. The linear wave is assumed based on the Airy wave theory in the present study. The water level of the wave is given as

$$\eta = \eta_0 \sin(\omega t - n_x x - n_y y) \tag{1}$$

where η_0 is the amplitude, $\omega = gk\tanh(kH)$, and $k = 2\pi/\lambda$. λ is the wavelength. n_x and n_y are the x and y components of the wave direction. The velocities of the fluid are given as

$$u_x = \left\{\omega\eta_0 \sin(\omega t - n_x x - n_y y)\frac{\cosh[k(z+H)]}{\sinh(kH)} + U_0\right\} n_x \tag{2}$$

$$u_y = \left\{\omega\eta_0 \sin(\omega t - n_x x - n_y y)\frac{\cosh[k(z+H)]}{\sinh(kH)} + U_0\right\} n_y \tag{3}$$

$$u_z = \omega\eta_0 \cos(\omega t - n_x x - n_y y)\frac{\sinh[k(z+H)]}{\sinh(kH)} \tag{4}$$

2.2.2 Morison model. The line-type elements of the fish cage system include the floating collar, sinker tube, mooring line and bridles. The normal and tangential forces resulting from the viscous effects are given by Equations (5) and (6).

$$\boldsymbol{F_n} = \frac{1}{2} C_n \rho L d |\boldsymbol{U_n}| \boldsymbol{U_n} \tag{5}$$

$$\boldsymbol{F_t} = \frac{1}{2} C_t \rho L \pi d |\boldsymbol{U_t}| \boldsymbol{U_t} \tag{6}$$

where the directions of the $\boldsymbol{F_n}$ and $\boldsymbol{F_\tau}$ are shown in Figure 3. L and d are the length and diameter of the line element, respectively.

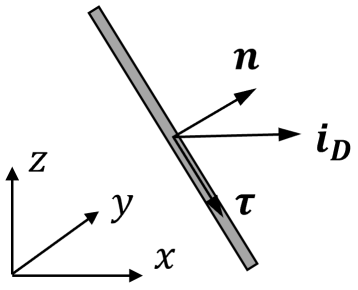

Figure 3. Schematic of the Morison model for the line-like elements.

The tangential and normal velocities are calculated as

$$\boldsymbol{U_t} = [(\boldsymbol{U} - \boldsymbol{v}) \cdot \boldsymbol{\tau}]\boldsymbol{\tau}, \qquad \boldsymbol{U_n} = (\boldsymbol{U} - \boldsymbol{v}) - \boldsymbol{U_t} \tag{7}$$

where $\boldsymbol{U}$ and $\boldsymbol{v}$ are the velocities of fluid and structure respectively, and $\boldsymbol{\tau}$ is the vector of the line element. $\boldsymbol{U}$ is given by Equations (2)-(4). C_n and C_t are normal and tangential drag coefficients, given by experimental results based on the Reynolds number of the line-type structures.

2.2.3 Screen model. The drag force $\boldsymbol{F_D}$ and lift force $\boldsymbol{F_L}$ are calculated as

$$\boldsymbol{F_D} = \frac{1}{2} C_D \rho A_t |\boldsymbol{U} - \boldsymbol{v}|^2 \boldsymbol{i_D}, \qquad \boldsymbol{F_L} = \frac{1}{2} C_L \rho A_t |\boldsymbol{U} - \boldsymbol{v}|^2 \boldsymbol{i_L} \tag{8}$$

where

$$\boldsymbol{i_D} = \frac{\boldsymbol{U} - \boldsymbol{v}}{|\boldsymbol{U} - \boldsymbol{v}|}, \qquad \boldsymbol{i_L} = \boldsymbol{i_D} \times \boldsymbol{n} \times \boldsymbol{i_D} \tag{9}$$

The values of C_D and C_L are given using the following the formulas [7].

$$C_D = 0.04 + (-0.04 + S_n - 1.24S_n^2 + 13.7S_n^3)\cos\theta \tag{10}$$

$$C_L = (0.57S_n - 3.54S_n^2 + 10.1S_n^3)\sin^2\theta \tag{11}$$

When the current passes one side of the net, the current velocity will decrease due to the friction on the net twines. The velocity reduction of the incoming flow is calculated using a reduction factor r [7-8,16],

$$r = 1 - 0.46C_{D(\theta=0)} \tag{12}$$

2.2.4 Strip model. The strip model is proposed to calculate the hydrodynamic force of the floating collars. The floating collars are divided into N circular sections and each section is a line-type element as discussed in Section 2.2.2. In each section, the water surface is assumed to be flat, as shown in Figure 4. Because the collar sections are not fully submerged, the hydrodynamic force in Equations (5) - (6) need to be corrected using a submerging factor κ_D.

$$\kappa_D = \begin{cases} 0, & \Delta z < -R \\ \frac{1}{2}\left(1 + \frac{\Delta z}{R}\right), & -R \le \Delta z \le R \\ 1, & \Delta z > R \end{cases} \tag{13}$$

where Δz is the distance from the undistributed water level to the centre of the section, R is the radius of the section and $\theta = \arccos\left(-\frac{\Delta z}{R}\right)$.

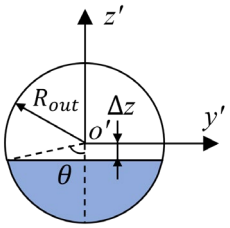

Figure 4. Illustrations of the strip mode for the floating collars.

2.3 Structural models

2.3.1 Extended position-based dynamics (XPBD). The structural responses of the net, mooring line and bridles are calculated using an XPBD method. In XPBD method, the positions of the nodes are updated based on the masses at the nodes and the stiffness k_j of the constraints between the nodes. After the nodes are updated using Newton's second law without considering the inner forces resulting from the constraints, the position update for the two nodes due to a single constraint C_j is given by evaluating the following expressions.

$$\boldsymbol{\Delta x_1} = +\Delta\lambda_j w_{j,1}\boldsymbol{q}$$
$$\boldsymbol{\Delta x_2} = -\Delta\lambda_j w_{j,2}\boldsymbol{q} \tag{14}$$

Where $\boldsymbol{\lambda} = [\lambda_1, \lambda_1, \cdots, \lambda_M]^T$ is the Lagrange multiplier of the constraints $\boldsymbol{C} = [C_1, C_1, \cdots, C_M]^T$. $w_{j,1}$ and $w_{j,2}$ are the inverse mass of the nodes. $\boldsymbol{q}$ is the unit vector between the two nodes. $\boldsymbol{\Delta\lambda}$ is the change of $\boldsymbol{\lambda}$, and can be given by Equation (15), where $\tilde{\alpha}_j = \frac{1}{k_j \Delta t^2}$.

$$\Delta\lambda_j = \frac{-C_j}{w_{j,1} + w_{j,2} + \tilde{\alpha}_j} \tag{15}$$

Compared with the mass spring method, XPBD can provide a quick result for the net dynamics in an implicit way. However, XPBD has its inevitable error for calculating the tensions of the constraints. It is because the masses of the nodes are involved when evaluating the Lagrange multiplier change. It is against the physics intuition that the elastic force is only determined by the stiffness and the constraint. If $w_{j,1}$ and $w_{j,2}$ are removed from the denominator of Equation (15), the method will become unstable. To correct the results of XPBD and maintain the stable update process, a PBD correction is proposed by applying extra forces acting on the two nodes of the constraint.

$$\boldsymbol{F_1} = +\gamma_j \boldsymbol{q} \qquad \boldsymbol{F_2} = -\gamma_j \boldsymbol{q} \tag{16}$$

where $\Delta\gamma_j$ is evaluated by Equation (17).

$$\gamma_j = \frac{-C_j\left(w_{j,1} + w_{j,2}\right)}{\left(w_{j,1} + w_{j,2} + \tilde{\alpha}_j\right)\tilde{\alpha}_j \Delta t^2} \tag{17}$$

2.3.2 Mode superposition (MS). The structural responses of the floating collars and sinker tube are calculated using the mode superposition method. The structures of the floating collars and sinker tube are simplified as 3D beam models, where the sections are shown in Figure 5. The conjunctions between the two floating collars are neglected for simplicity, and the two floating collars are assumed to be a single circular beam. The section information of the floating collars and sinker tube are listed in Table 3. To address the inertia forces due to the added mass and additional mass of the water (see Figure 5b), the mass of each beam element includes the contributions the added mass of water with an added mass coefficient of $C_a = 1$. while that of the sinker tube includes the contributions of the added mass and the additional mass of water.

Table 3. Section information of the floating collars and sinker tube.

Section	E (GPa)	$G\ (GPa)$	A (m^2)	J (m^4)	I_y (m^4)	I_z (m^4)
Floating collars	3	0.6	0.044	0.0068	6.2×10^{-4}	0.0062
Sinker tube	3	0.6	0.015	2×10^{-4}	1×10^{-4}	1×10^{-4}

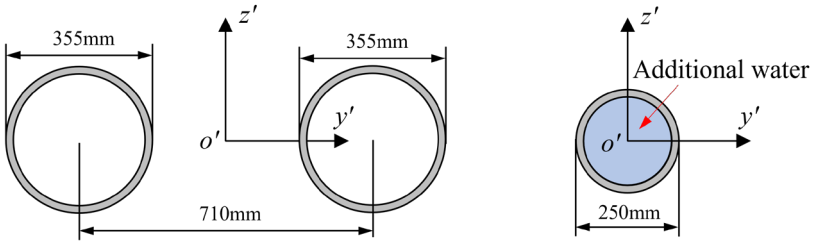

(a) Floating collars' section (b) Sinker tube's section

Figure 5. Descriptions of the floating collars' and sinker tube's sections.

The modal coordinate is updated based on the Newmark-beta method.

$$q_j^{(n+1)} = P_j / K_j \tag{18}$$

where

$$P_j = F_j^{(n)} + a_0 q_j^{(n)} + a_2\, \dot{q}_j^{(n)} + a_3\, \ddot{q}_j^{(n)} \tag{19}$$

$$K_j = a_0 + \left(2\pi f_j\right)^2 \tag{20}$$

The updates of the acceleration and speed are given as

$$\ddot{q}_j^{(n+1)} = a_0\left(q_j^{(n+1)} - q_j^{(n)}\right) - a_2\, \dot{q}_j^{(n)} - a_3\, \ddot{q}_j^{(n)} \tag{21}$$

$$\dot{q}_j^{(n+1)} = \dot{q}_j^{(n)} + a_6 \ddot{q}_j^{(n)} + a_7 \ddot{q}_j^{(n+1)} \tag{22}$$

The modal force is calculated as

$$F_j^{(n)} = \sum_{i=1}^{N} \boldsymbol{\phi}_{i,j} \cdot \boldsymbol{F}_i \tag{23}$$

where $\boldsymbol{F}_i$ is the external force vector acting on the i^{th} node. $\boldsymbol{\phi}_{i,j}$ is the shape function vector at the i^{th} node. The parameters of a_0, a_2, a_3, a_6 and a_7 are given as $a_0 = \frac{1}{\beta \Delta t^2}$, $a_2 = \frac{1}{\beta \Delta t}$, $a_0 = \frac{1}{2\beta} - 1$, $a_6 = \Delta t(1-\gamma)$, and $a_7 = \Delta t\gamma$, where $\beta = 1/4$ and $\gamma = 1/2$. The updates of the node positions and speeds are given by evaluating the following expressions.

$$\boldsymbol{x}_i^{(n+1)} = \boldsymbol{x}_{0,i} + \sum_{j=1}^{N} \boldsymbol{\phi}_{i,j}\, q_j^{(n+1)} \tag{24}$$

$$\boldsymbol{u}_i^{(n+1)} = \boldsymbol{u}_{0,i} + \sum_{j=1}^{N} \boldsymbol{\phi}_{i,j}\, q_j^{(n+1)} \tag{25}$$

2.3.3 Coupling between XPBD and MS. The coupling between XPBD and MS is conducted as follows.

(1) XPBD provides the tensions of the brindles and the net ropes for MS.
(2) MS provides the positions and speeds of the nodes located at the centre lines of the floating collars and sinker tube.

In the present study, the XPBD and MS share the same nodes at the centre lines of the floating collars and sinker tube. For XPBD, the inverse masses of these nodes are set to be zero, which means that their positions and speeds are not updated in XPBD. These motions are updated by the MS solver. For the MS solver, the tensions of the brindles and the net ropes are provided by XPBD.

3. Results and discussions

3.1 Case description

The rough sea condition is simplified as the waves with a heigh of 156 m [17] and a current with a speed of 1m/s. The water depth is 100 m. The wave period is 10 s. The free surface and the velocities of the incoming waves can be given by Equations (1) – (4) using the Airy wave theory. The initial locations of the fish cages on the water surface and in deep water in a current with a speed of 0.3m/s are shown in Figure 6. The total simulation time is 300 s, which includes 30 wave periods.

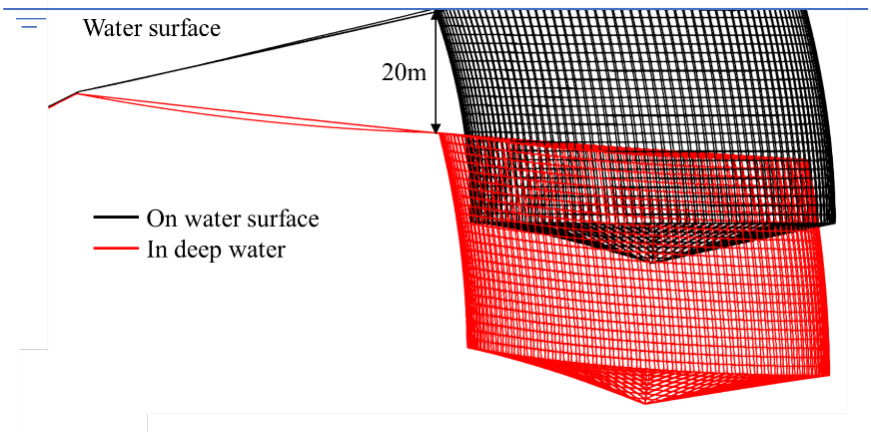

Figure 6. Fish cages on water surface and in deep water in a current with a speed of 0.3 m/s.

3.2 Dynamic process

Figure 7 shows the time-step sensitivity study of the horizontal force of the fish cage on the water surface. Three time-steps of 0.5 ms, 1 ms and 2 ms are tested. The results of 0.5 ms and 1 ms exhibit a good agreement, indicating that the convergent result is achieved when the time step is small as 1ms. Table 4 shows the computational time of the surface cases with the three time-steps. As the time-step decreases, the computational time has a rapid increase. Therefore, to achieve a balance between the accuracy and computational cost, the time-step of 1ms is selected for further calculations.

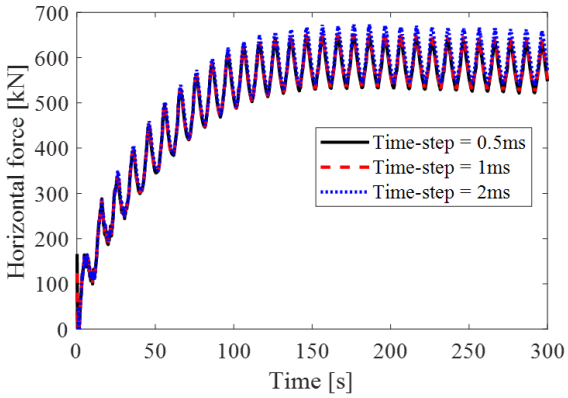

Figure 7. Time-step sensitivity study of the horizontal force of the fish cage on the water surface.

Table 4. Computational time of the surface case with different time-steps

Time-step (ms)	0.5	1.0	2.0
Computational time (s)	4185	1856	937

Figure 8 shows the comparisons of the horizontal force between the fish cages on the water surface and in deep water. The horizontal force has a significant reduction when the fish cage submerges to the deep water. The comparisons of the average results and the variation of the horizontal forces are shown in Table 4. When the fish cage is lowered by 20 m from the water surface, both the average results and the variation of the horizontal forces are significantly reduced.

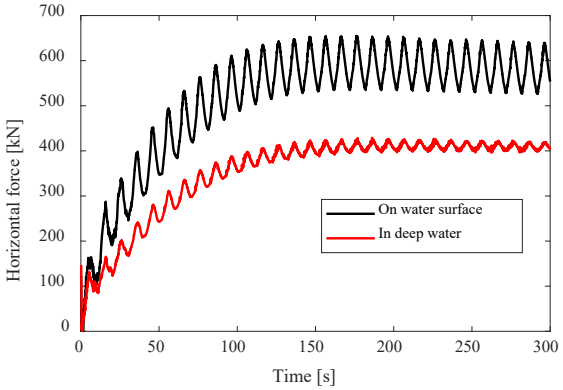

Figure 8. Comparisons of the horizontal force between the fish cages on the water surface and in deep water.

Table 5 Comparisons of the average results and the variation of the horizontal forces.

	On water surface	In deep water	Reduction
Average horizontal force (kN)	581	408	30%
Horizontal force variation (kN)	113	21.2	81%

Figure 9 shows the comparisons of the deformations between the fish cages on water surface and in deep water in a typical period from 290 s to 300 s. The deformation of the floating collars of the fish cage on water surface is much larger than that in deep water, which indicates that the floating collars of the fish cage on the water surface experience larger stress than that in deep water.

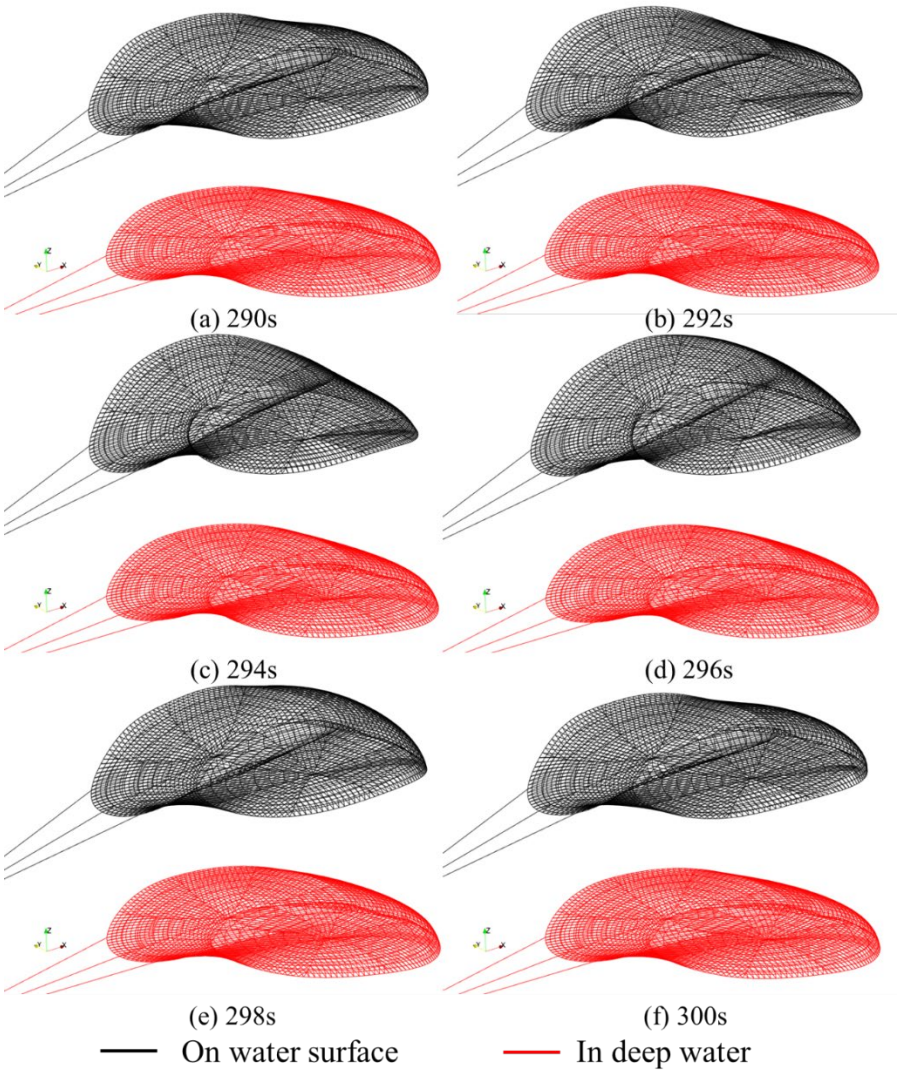

Figure 9. Comparisons of the deformations between the fish cages on the water surface and in deep water.

4. Conclusion

The dynamic responses of a single point mooring submersible fish cage in waves and current are assessed using numerical methods. The wave and current conditions are modelled using the airy wave theory. For the floating collars and sinker tube, the Morison model is adopted to calculate the hydrodynamic force and the modal superposition method is proposed for the structural response calculations. For the aquaculture nets, the screen model is adopted to compute the hydrodynamic force and the XPBD method is proposed to obtain the structural deformations. The hydrodynamic forces and the deformations of the fish cages are compared between the fish cage on water surface and in deep water. Results show that lowering the fish cage by 20m from the water surface leads to a 30% reduction in average horizontal force and an 81% decrease in the variation of horizontal force. Additionally, significant reductions in the deformation of the floating collars are observed. Consequently, using

submersible fish cages can effectively mitigate physical stress and prevent structural damage for the fish cage system.

It should be mentioned that more cases should be performed, and more structural information should be provided to show the differences between the surface case and the deep-water case. The further study will also focus on the structural responses of the descending and ascending of the fish cage. In addition, the coupling of XPBD and MS can provide a quick solution for the structural modelling of the fish farm system, which can be utilized at the initial stage of fish farm design.

Acknowledgment: This study was supported by the Research Council of Norway through the project "Unleashing the sustainable value creation potential of offshore ocean aquaculture" (Project number: 328724).

References

[1] FAO, 2018. In: The State of World Fisheries and Aquaculture 2018 Meeting the sustainable development goals. Rome. Licence: CC BY-NC-SA 3.0 IGO.
[2] Cardia, F., Lovatelli, A., 2015. Aquaculture Operations in Floating HDPE Cages: A Field Handbook. FAO and Ministry of Agriculture of the Kingdom of Saudi Arabia.
[3] Li, L., Fu, S.X., Xu, Y.W., Wang, J.G., Yang, J.M., 2013. Dynamic responses of floating fish cage in waves and current. *Ocean. Eng.* **72**, 297–303.
[4] Moe-Føre, H., Lader, P., Lien, E., Hopperstad, O., 2016. Structural response of high solidity net cage models in uniform flow. *J. Fluids Struct.* **65**, 180–195.
[5] Cheng, H., Li, L., Aarsæther, K. G., Ong, M. C., 2020. Typical hydrodynamic models for aquaculture nets: A comparative study under pure current conditions. Aquacultural Engineering, 90, 102070.
[6] Fridman, A.Lv., 1973. Theory and Design of Commercial Fishing Gear (Trans. from Russ.). Jerusalem.
[7] Aarsnes, J.V., Løland, G., Rudi, H., 1990. Current Forces on Cage, Net Deflection. Eng. Offshore Fish Farm. p. 891–921.
[8] Løland, G., 1991. Current Forces on and Flow Through Fish Farms. *PhD Thesis,* Norwegian Institute of Technology.
[9] Zhao, Y. P., Bi, C. W., Dong, G. H., Gui, F. K., Cui, Y., Guan, C. T., Xu, T. J., 2013. Numerical simulation of the flow around fishing plane nets using the porous media model. *Ocean Eng. 62*, 25-37.
[10] Chen, H., Christensen, E. D., 2017. Development of a numerical model for fluid-structure interaction analysis of flow through and around an aquaculture net cage. *Ocean Eng.* **142,** 597-615.
[11] Cifuentes, C., Kim, M.H., 2017. Numerical simulation of fish nets in currents using a Morison force model. *Ocean. Syst. Eng.* **7**(2), 143–155.
[12] Berstad, A.J., Aarsnes, J.V., 2018. A case study for an offshore structure for aquaculture: comparison of analysis with model testing. *ASME 2018 37th Int. Conf. Ocean, Offshore Arctic Eng.: American Society of Mechanical Engineers* V11BT12A057-V11BT12A057.
[13] Xu, T. J., Zhao, Y. P., Dong, G. H., Gui, F. K. 2013. Analysis of hydrodynamic behavior of a submersible net cage and mooring system in waves and current. *Appl. Ocean Res.* **42**, 155-167.
[14] Müller, M., Heidelberger, B., Hennix, M., Ratcliff, J. 2007. Position based dynamics. *J. Visual Commun. Image Repr.* **18**(2), 109-118.
[15] Miles, M., Müller, M., Chentanez, N., 2016. XPBD: position-based simulation of compliant constrained dynamics. *Proc. 9th Int. Conf. Motion in Games.* P. 49 - 54
[16] Kristiansen, T., Faltinsen, O. M., 2012. Modelling of current loads on aquaculture net cages. *J. Fluids Struct.* **34**, 218–235.
[17] Lee, C. W., Lee, G. H., Choe, M. Y., Song, D. H., Hosseini, S. A., 2009. Dynamic behavior of a submersible fish cage. In: *Int. Conf. Offshore Mech. Arctic Eng.* **43444**, 201-206.